

# Mechanical properties and microstructure of a $\text{Si}_3\text{N}_4/\text{Ti}_3\text{SiC}_2$ multilayer composite

Luo Yong-Ming\*, Pan Wei, Li ShuQin, Chen Jian, Wang RuiGang, Li JianQiang

State Key Lab of New Ceramics and Fine Processing, Department of Materials Science and Engineering Tsinghua University, Beijing 100084, China

Received 30 July 2001; received in revised form 9 August 2001; accepted 27 September 2001

## Abstract

A new  $\text{Si}_3\text{N}_4/\text{Ti}_3\text{SiC}_2$  laminated composite which was manufactured by the powder metallurgy method is presented. The work of fracture was measured in four-point bending at a crosshead speed of 0.05 mm/min. The results show that the mechanical properties of multilayered composites consisting of  $\text{Ti}_3\text{SiC}_2$  layers in  $\text{Si}_3\text{N}_4$  were significantly enhanced. Three-step toughening behaviors were found in the material. The crack deflection is regarded as a dominant toughening mechanism, meanwhile the unique microstructure and properties of  $\text{Ti}_3\text{SiC}_2$  contributed to the improvement, thus preventing catastrophic failure. © 2002 Elsevier Science Ltd and Techna S.r.l. All rights reserved.

**Keywords:** B. Microstructure; C. Mechanical properties;  $\text{Si}_3\text{N}_4/\text{Ti}_3\text{SiC}_2$ ; Multilayer composites

## 1. Introduction

Silicon nitride is considered a potentially useful structural ceramic for its combination of toughness, strength, hardness, and chemical and thermal durability. Unfortunately, the lack of its reliability in mechanical properties has been a critical problem preventing widespread structural applications. Cook et al. [1] suggested that this problem can be overcome by introducing weak interfaces to deflect a growing crack. Following Cook's idea  $\text{Si}_3\text{N}_4$  ceramic composites with a layered structure have been evaluated [2–7]. These layered composites were reported to present several improved properties (e.g. increase in fracture toughness, crack arrest, multiple cracking, and so forth). To overcome the lack of reliability, the features of layered composites are especially attractive.

In this paper we have successfully fabricated  $\text{Si}_3\text{N}_4/\text{Ti}_3\text{SiC}_2$  multilayer ceramic by powder metallurgy and hot-pressing. It is well known that  $\text{Ti}_3\text{SiC}_2$  is a novel structural/functional material. Hexagonal  $\text{Ti}_3\text{SiC}_2$  has a layer structure on the atomic scale. Recent studies show that  $\text{Ti}_3\text{SiC}_2$  combines the merits of both ceramics and metals, such as being electrically and thermally conductive, as well as easy to machine and resistant to thermal

shock, high strength, high toughness, high melting points, low density and thermal stability [8–15]. Thus  $\text{Ti}_3\text{SiC}_2$  is considered to be effective to overcome the lack of reliability. In present research we selected  $\text{Ti}_3\text{SiC}_2$  as the weak interface to improve the  $\text{Si}_3\text{N}_4$  toughness without sacrifice the silicon nitride ceramic properties. The microstructure and mechanical properties of the  $\text{Si}_3\text{N}_4/\text{Ti}_3\text{SiC}_2$  multilayer ceramic have been evaluated.

## 2. Experimental procedure

### 2.1. Raw materials and fabrication processing

$\text{Si}_3\text{N}_4$  powder (E-10, UBE Industries, Tokyo, Japan) with MgO (8 mass%, from Shin-etsu Chemical Co., Tokyo, Japan, 99.99% pure) and  $\text{CeO}_2$  (2 mass%, from Shin-etsu Chemical Co., Tokyo, Japan, 99.99% pure) were ball-milled in ethanol for 48h. The slurry was stirred-drying with rotary evaporator at 60 °C, the mixture was reground in a mortar and pestle and screened through a 100-mesh sieve.  $\text{Ti}_3\text{SiC}_2$  powder was synthesized directly from elemental titanium, silicon, and graphite powders with solid-liquid method at 1270 °C. Pure  $\text{Ti}_3\text{SiC}_2$  powders were obtained [16] by first removing  $\text{TiSi}_2$  using HF solution, and then heating the powders in air at 500 °C for 5 h, finally washing the powders with hot

\* Corresponding author.

E-mail address: lym98@mails.tsinghua.edu.cn (L. YongMing).

$(\text{NH}_4)_2\text{SO}_4 + \text{H}_2\text{SO}_4$  solution. The resulting powder had average particle size  $1.0\text{ }\mu\text{m}$  (purity higher 98%). The dried  $\text{Ti}_3\text{SiC}_2$  and  $\text{Si}_3\text{N}_4$  starting mixtures were carefully weighed and alternately layered in a steel die ( $\Phi 50\text{ mm}$  inner diameter) in a sequence of  $\text{Si}_3\text{N}_4/\text{Ti}_3\text{SiC}_2/\text{Si}_3\text{N}_4/\text{Ti}_3\text{SiC}_2/\dots/\text{Si}_3\text{N}_4$ , then were compressed at  $100\text{ MPa}$ . The layer thickness of  $\text{Si}_3\text{N}_4$  and  $\text{Ti}_3\text{SiC}_2$  were  $0.30$  and  $0.15\text{ mm}$ , respectively. The green compact was hot-pressed in graphite dies at  $25\text{ MPa}$  under flowing argon at  $1600\text{ }^\circ\text{C}$  for  $2\text{ h}$ . The heating and cooling rates were  $10$  and  $15\text{ }^\circ\text{C/min}$ , respectively.

## 2.2. Characterization

Specimens for flexural tests were cut and ground from the billets to nominal dimensions of  $4\times 3\times 36\text{ mm}$ . Flexure strength was measured in a three-point bending test with spans of  $30\text{ mm}$  at a crosshead speed of  $0.5\text{ mm/min}$ . The prospective tensile surfaces were ground and polished to achieve a mirrorlike surface finish prior to mechanical testing. The work of fracture was measured in four-point bending test with outer and inner spans of  $40$  and  $20\text{ mm}$ , respectively. The bending tests

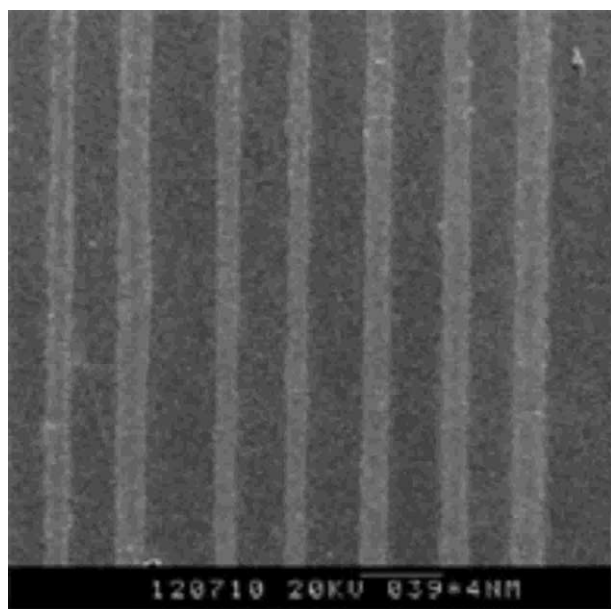
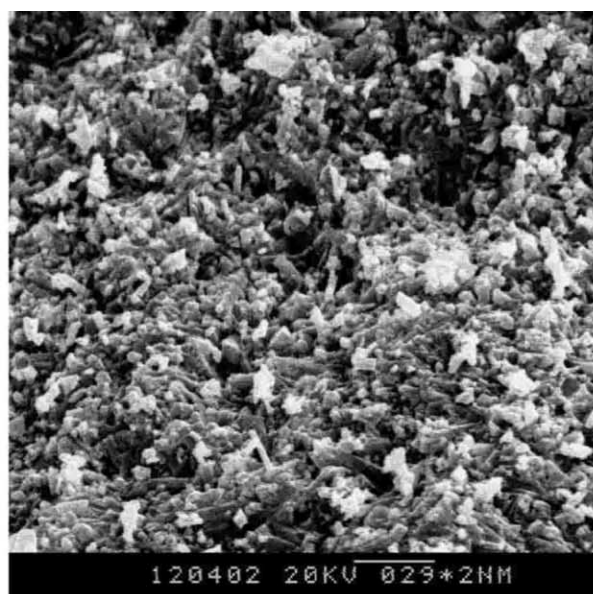
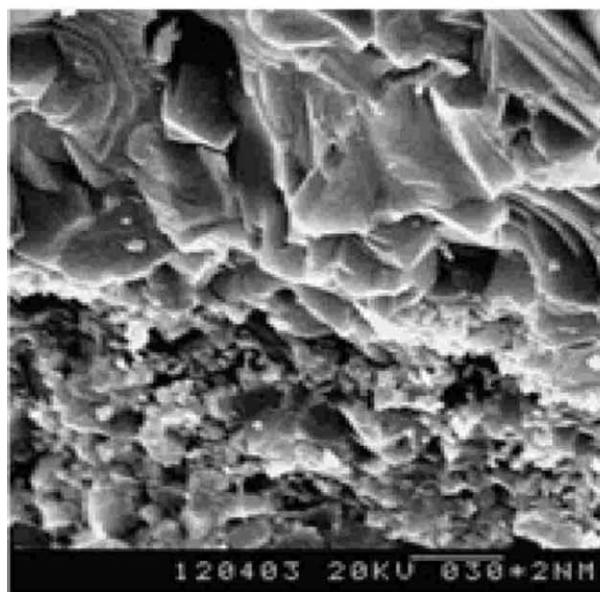


Fig. 1. Macrograph of the laminated composite  $\text{Si}_3\text{N}_4/\text{Ti}_3\text{SiC}_2$ .



(a)



(b)

Fig. 3. SEM of the fracture surface of  $\text{Si}_3\text{N}_4/\text{Ti}_3\text{SiC}_2$  laminated composites: (a)  $\text{Si}_3\text{N}_4$  layer; (b)  $\text{Ti}_3\text{SiC}_2$  layer.

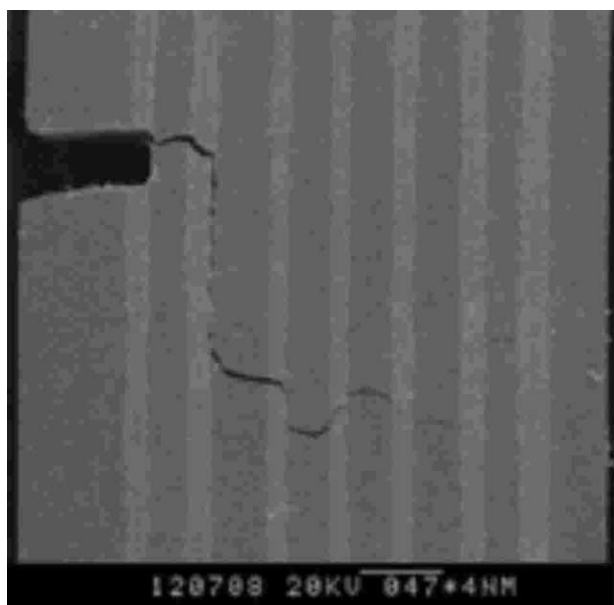


Fig. 2. Crack propagation in the laminated composite  $\text{Si}_3\text{N}_4/\text{Ti}_3\text{SiC}_2$ .

were performed at a crosshead speed of 0.05 mm/min. The work of fracture of each specimen was calculated by determining the area under the load-crosshead deflection curve and dividing it by twice the cross-sectional area of the sample. The fracture surface of the laminated composites were examined by scanning electron microscope (SEM). Energy-dispersive X-ray analysis was used to qualitatively display the compositional distribution in the laminated composites.

### 3. Results and discussion

The mechanical properties were measured using the hot-pressed laminated sample. The work of fracture of  $\text{Si}_3\text{N}_4/\text{Ti}_3\text{SiC}_2$  laminated composites was  $4760 \text{ J/m}^2$ , and the flexure strength was  $746.3 \pm 10.2 \text{ MPa}$ , while work of the fracture of  $\text{Si}_3\text{N}_4$  ceramic was only  $100 \text{ J/m}^2$ . The work of the fracture of  $\text{Si}_3\text{N}_4/\text{Ti}_3\text{SiC}_2$  laminated composites was higher than that of  $\text{Si}_3\text{N}_4$  monolithic materials. Accordingly  $\text{Ti}_3\text{SiC}_2$  increased reliability of  $\text{Si}_3\text{N}_4$  ceramic in mechanical properties when it was interface layer, thus preventing catastrophic failure.

On a four-point bending test fixture, conventional ceramics fail by tensile cracking. In contrast, these multilayer ceramics with low interface shear strength could fail by a combination of shear and tensile cracking. The maximum tensile stress in a four-point-bend bar can be expressed as [17]

$$\sigma_{t,\max} = \frac{3ap}{bh^2} \quad (1)$$

where  $p$  is the load,  $a$  is the distance between the inner and outer loading points,  $b$  is width, and  $h$  is the thickness of the bar. The relationship between the maximum shear stress and the maximum tensile stress for the four-point load condition can be written as [17]

$$\frac{\tau_{\max}}{\sigma_{t,\max}} = \frac{h}{4a} \quad (2)$$

Shear fracture will occur in these specimens if the maximum shear stress exceeds the shear strength of the interface layer. Based on these considerations, the fracture behavior of a multiplayer ceramic in a bending test depends not only on the microstructure but also on the specimen geometry. The shear cracking would make the specimen more compliant in bending, therefore relieving some of the tensile stresses.

Fig. 1 shows their structure of  $\text{Si}_3\text{N}_4/\text{Ti}_3\text{SiC}_2$  laminated composites. The silicon nitride layers appear gray and the  $\text{Ti}_3\text{SiC}_2$  interfaces appear as thin, bright layers separating the  $\text{Si}_3\text{N}_4$  layers. Fig. 2 shows a typical crack propagation manner of the hot-pressing laminated composite. As shown in Fig. 2, a major tensile crack propagates through the specimen although it is deflected by  $\text{Ti}_3\text{SiC}_2$  layers. One remarkable feature observed in Fig. 2 is the interlocking of toothlike, debonded layers. This indicates that the maximum shear stress must exceed the shear strength of the  $\text{Ti}_3\text{SiC}_2$  layer.

Fig. 3 shows the micrographs of  $\text{Si}_3\text{N}_4/\text{Ti}_3\text{SiC}_2$  laminated composites specimen fractured at room temperature. Whisker like  $\beta\text{-Si}_3\text{N}_4$  is clearly seen in the  $\text{Si}_3\text{N}_4$  layer, which indicates  $\alpha\text{-Si}_3\text{N}_4$  has transformed to the  $\beta\text{-Si}_3\text{N}_4$  phase, but sintered temperature was rather

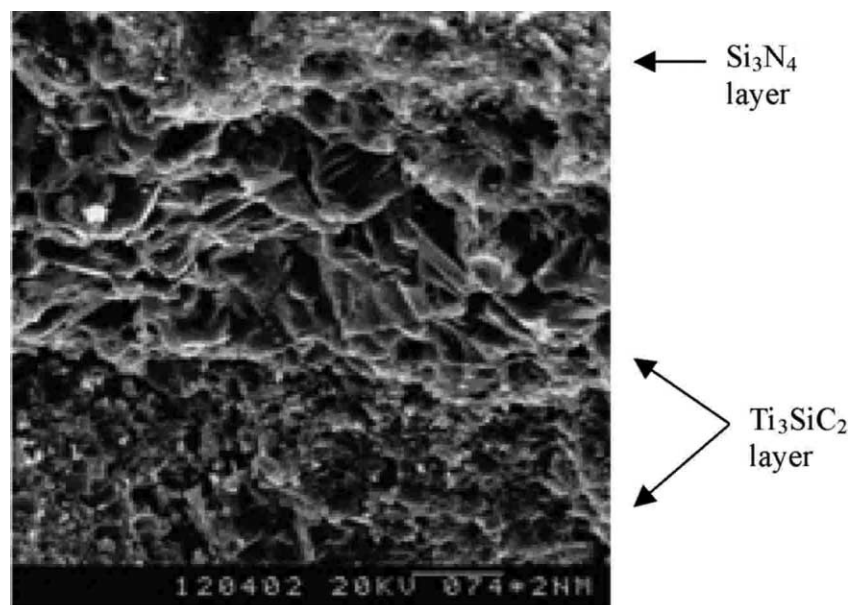


Fig. 4. SEM of  $\text{Ti}_3\text{SiC}_2$  grains in different positions.

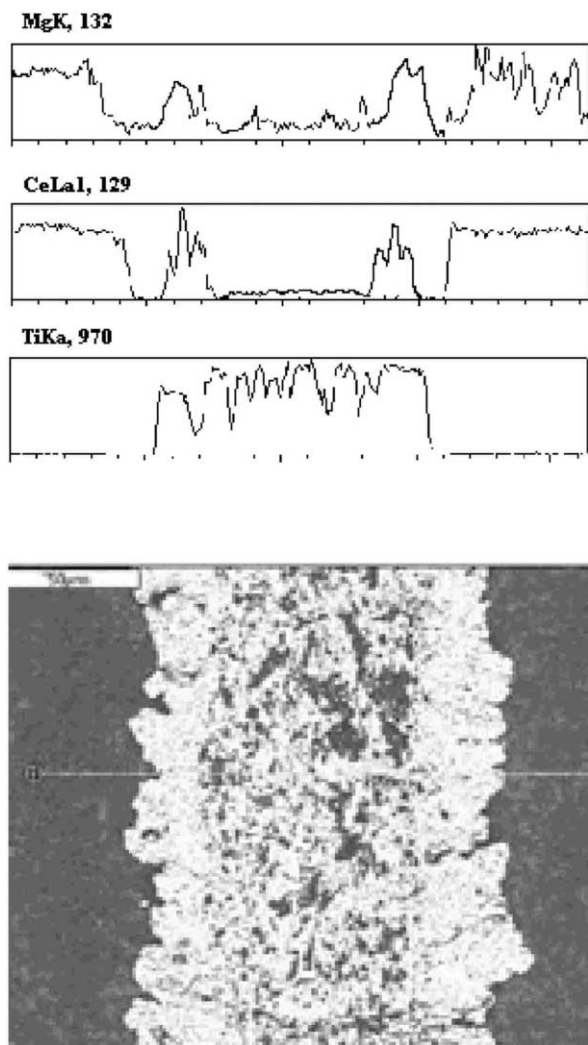


Fig. 5. Element distribution in the laminated composites material.

lowly, so size of the  $\beta$ - $\text{Si}_3\text{N}_4$  grains was small. The characteristic of the laminated  $\text{Ti}_3\text{SiC}_2$  grains can easily be identified in these micrographs. Upon analysis of the fracture surface, the failure in the  $\text{Ti}_3\text{SiC}_2$  layers appears to be intergranular in nature while exhibiting a highly layered structure. This feature along with the rough nature of the fracture surface has led to the suggestion that this ceramic possesses a weak interface that leads to a behavior of a nanolaminate [18,19]. It is seen that pull-out of  $\text{Ti}_3\text{SiC}_2$  grains is evidence. Micro-plastic deformation can be seen in such region, which may act more effectively as an energy-absorbing mechanism and toughen the material further.

In the microstructure of laminated composites we found that the size of the  $\text{Ti}_3\text{SiC}_2$  grains near the  $\text{Si}_3\text{N}_4$  layer was bigger than for those removed from the  $\text{Si}_3\text{N}_4$  layer (see Fig. 4). Qualitative energy-dispersive X-ray microanalysis was used to detect the element distribution in the laminated composites material (see Fig. 5). Fig. 5 shows the Mg, Ce and Ti element line map of the region of the laminated material. We found that the Ce

and Mg elements have diffused in fringe of  $\text{Ti}_3\text{SiC}_2$  layers. This indicates that during the sintered process produced liquid in  $\text{Si}_3\text{N}_4$  layers diffused to  $\text{Ti}_3\text{SiC}_2$  layers and accelerated growth of the size of  $\text{Ti}_3\text{SiC}_2$  grains.

#### 4. Conclusions

New  $\text{Si}_3\text{N}_4/\text{Ti}_3\text{SiC}_2$  laminated composites have been manufactured by powder metallurgy method. Multilayer materials have shown noncatastrophic failure in four-point bend tests. The three-step toughening behavior observed is a fundamental appearance in  $\text{Si}_3\text{N}_4/\text{Ti}_3\text{SiC}_2$  laminated composites. Crack deflection along the weak interfaces was thought to be the major mechanism for improving fracture resistance. The secondary toughening behavior seems to be the layer structure of  $\text{Ti}_3\text{SiC}_2$  on the atomic scale, pull-out and micro-plastic deformation of  $\text{Ti}_3\text{SiC}_2$  grains. The difference size of  $\text{Ti}_3\text{SiC}_2$  grains was tertiary toughening behavior. Multiple toughening mechanisms obviously enhanced fracture resistance. The average apparent work of fracture of the laminated composites was about  $4760 \text{ J/m}^2$ .

#### References

- [1] J. Cook, J.E. Gordon, Proc. Roy. Soc. London A282 (1964) 508.
- [2] H.-y. Liu, S.M. Hsu, J. Am. Ceram. Soc. 79 (1996) 2452.
- [3] S. Baskaran, S. Nunn, D. Popovic, J.W. Halloran, J. Am. Ceram. Soc. 76 (1993) 2209.
- [4] D. Popovic, S. Baskaran, G. Zywicki, C. Arens, J.W. Halloran, in: B.W. Sheldon, S.C. Danforth (Eds.), Silicon-Based Structural Ceramics, vol. 42, American Ceramic Society, Westerville, OH, 1994, p. 173.
- [5] P. Sajgalik, Z. Lences, J. Dusza, in: D.S. Yan, R. Fu, S.X. Shi (Eds.), Proceedings of the 5th International Symposium on Ceramic Materials and Components for Engines (Shanghai, China May 1994), World Scientific Publishing, Singapore, 1995, p. 198.
- [6] Yasuhiro Shigegaki, J. Am. Ceram. Soc. 79 (1996) 2197.
- [7] P. Wei, et al., Mater. Lett., in press.
- [8] Y.P. Zeng, D.I. Jiang, T. Watanabe, J. Am. Ceram. Soc. 83 (2000) 2999.
- [9] J.J. Nickl, K.K. Schweitzer, P. Luxenberg, J. Less-Common Metals 26 (1972) 335.
- [10] R. Pampuch, J. Lis, L. Stobierski, M. Tymkiewicz, J. Eur. Ceram. Soc. 5 (1989) 283.
- [11] T. El-Raghy, M.W. Barsoum, A. Zavalangos, S. Kalidindi, J. Am. Ceram. Soc. 82 (1999) 2855.
- [12] M.W. Barsoum, T. El-Raghy, J. Am. Ceram. Soc. 79 (1996) 1953.
- [13] T. El-Raghy, A. Zavalangos, M.W. Barsoum, S. Kalidindi, J. Am. Ceram. Soc. 80 (1997) 513.
- [14] I.M. Low, S.K. Lee, B. Lawn, M.W. Barsoum, J. Am. Ceram. Soc. 81 (1998) 225.
- [15] T. Goto, T. Harai, Mater. Res. Bull. 22 (1987) 1195.
- [16] C. Racault, F. Langlais, R. Naslain, J. Mater. Sci. 29 (1994) 3384.
- [17] J.V. Mullin, A.C. Knoell, Basic concepts in composite beam testing, Mater. Res. Stand. (1970) 16–20.
- [18] M.W. Barsoum, T. El-Raghy, J. Am. Ceram. Soc. 79 (1996) 1953.
- [19] M.W. Barsoum, T. El-Raghy, J. Mater. Synth. Proc. 5 (1997) 197.